DOI: 10.1002/ejic.201100877

Electronic, Steric, and Ligand Influence on the Solid-State Structures of Substituted Sodium and Potassium Anilides

Carsten Glock,[a] Helmar Görls,[a] and Matthias Westerhausen*[a]

Keywords: Sodium / Potassium / Amides / Anilides / Metalation / Transamination reactions

Alkali metal amides are widely used as starting materials in salt metathesis and metalation reactions. *N*-Substituted anilides (phenylamides) of sodium and potassium AN(Ph)R [A = Na, K; R = methyl (Me), isopropyl (*i*Pr), phenyl (Ph)] are accessible by transamination with $AN(SiMe_3)_2$. Neutral coligands, such as ethers and amines, have a strong influence on the solid-state structures and solubility in common organic solvents. The crystal structures of the following anilides are discussed: $[(pmdta)KNPh_2]_2$ (**1**) (pmdta = *N*,*N*,*N*′,*N*′′,*N*′′-pentamethyldiethylenetriamine), $[(pmdta)KN(Ph)iPr]_2$ (**2**), $[(thf)_2NaNPh_2]_2$ (**3**) (thf = tetrahydrofuran), [(dme)NaN(Ph)-*i*Pr]$_2$ (**4**) (dme = 1,2-dimethoxyethane), $[(pmdta)NaNPh_2]_2$ (**5**), $[(thf)_2NaN(Ph)iPr]_2$ (**6**), $[(tmeda)NaN(Ph)iPr]_2$ (**7**) (tmeda = *N*,*N*,*N*′,*N*′-tetramethylethylenediamine), $[(dme)_2KN(Ph)iPr]_2$ (**8**), $[(diox)_{1.33}NaNPh_2]_\infty$ (**9**) (diox = 1,4-dioxane), [(diox)-NaN(Ph)*i*Pr]$_\infty$ (**10**), $[KN(Ph)Me]_\infty$ (**11**), $[\{(thf)KN(Ph)iPr\}_5]_\infty$ (**12**), $[\{(thf)KN(Ph)iPr\}_2{\cdot}2KN(Ph)iPr]$ (**13**), and $[(dme)_{0.25}KN-(Ph)iPr]_\infty$ (**14**). All of the sodium anilides contain a central four-membered Na_2N_2 ring, whereas the interactions between the cations and the π-systems of the phenyl groups have an increased importance in the potassium derivatives. Bidentate ether bases such as diox and dme can act as bridging ligands; however, this coordination behavior was not observed for the multidentate amines tmeda and pmdta.

Introduction

Alkali metal amides (MNR_2), especially lithium amides, are predominantly used in deprotonative metalation reactions due to their high Brønsted basicity and low nucleophilicity [NR_2 = diisopropylamide, bis(trimethylsilyl)amide, and 2,2,6,6-tetramethylpiperidide (tmp)].[1] Furthermore, alkali metal amides are used routinely for the metathetical synthesis of a variety of metal amides of transition metals as well as lanthanoids and actinoids.[2] The salt metathesis reaction represents a powerful and valuable tool to prepare substituted calcium bis(anilides),[3] highly reactive dialkylamides of calcium $[(tmeda)Ca(NR_2)_2]$ (NR_2 = tmp, N*i*Pr$_2$),[4,5] yttrium $[Y(tmp)_3]$, cerium $[(thf)Ce(tmp)_3]$,[6] and lanthanum $[(py)_3La(Cp''')(NR_2)_2]$ {Cp′′′ = [η^5-C_5H_2-1,2,4-$(SiMe_3)_3$], py = pyridine},[7] and heteroleptic organocalcium compounds such as $[(thf)_3Ca(Ph)\{N(SiMe_3)_2\}]$.[8] However, the metathetical approach to calcium bis(amides) from KNR_2 and CaI_2 must adhere to a strict stoichiometry in order to avoid undesirable byproducts.[8] An excess of potassium amide leads to the formation of potassium tris(amino)calciates, whereas a deficit of KNR_2 yields halide-containing substances.

Depending on the stoichiometry, the *N*-bound groups, and the reaction conditions (e.g. solvent and reaction temperature), several cases can be distinguished for the reaction of alkaline earth metal dihalides AeX_2 with alkali metal amides ANR_2 (A = alkali and Ae = alkaline earth metal): (i) The exact 1:2 stoichiometry yields $Ae(NR_2)_2$ (in addition to 2 equiv. of AX), which can aggregate and can contain alkaline earth metal centers coordinatively saturated by neutral coligands, such as ethers or amines, mainly depending on the solvent. Due to the fact that KI is insoluble in common organic solvents, this reaction usually is quantitative when KNR_2 is used as the starting material. (ii) Excess ANR_2 can lead to the formation of heterodimetallic complexes, which can be regarded as alkaline earth metalates of the types $A[Ae(NR_2)_3]$ and $A_2[Ae(NR_2)_4]$.[4,9–11] (iii) These alkaline earth metalates can dissociate and, depending on the equilibrium constant, the amounts of homometallic ANR_2 and $Ae(NR_2)_2$ in the reaction mixture can vary.

A substoichiometric 1:1 approach that used calcium diiodide and potassium amide yielded minor amounts of heteroleptic Hauser-type base $[(tmeda)Ca(tmp)(\mu\text{-}I)]_2$, which was also obtained from a Schlenk-type equilibrium of CaI_2 and $[(tmeda)Ca(tmp)_2]$.[5] However, this equilibrium is strongly shifted in favor of the homoleptic calcium complexes. This is in contrast to the behavior of classic Hauser bases, R_2N–Mg–X (NR_2 = tmp or N*i*Pr$_2$), which are stable for several hours in hot THF,[12,13] whereas Li(tmp) decomposes at 0 °C in THF solution.[14] Furthermore, the addition of small amounts of LiCl to lithium diisopropylamide enhances the reactivity significantly[15] and leads to the concept of Turbo–Hauser bases.[16]

[a] Institut für Anorganische und Analytische Chemie,
Friedrich-Schiller-Universität Jena
Humboldtstrasse 8, 07743 Jena, Germany
Fax: +49-3641-948102
E-mail: m.we@uni-jena.de

Supporting information for this article is available on the WWW under http://dx.doi.org/10.1002/ejic.201100877.

Inverse crowns represent another important class of amido-based deprotonation reagents that consist of an equimolar mixture of an alkali metal amide and a metal(II) bis(amide) where M^{II} is magnesium, manganese, or zinc.[13,17] The major structural motif is an eight-membered $(N–A–N–M^{II})_2$ ring. Larger inverse crown rings are formed when large substrate molecules, such as benzene, toluene, or ferrocene, are doubly deprotonated.

Alkali metal amides have experienced a significant broadening of application and, hence, an intensified entry into s-block metal chemistry. Despite the fact that the reactivity of these reagents can be adjusted to meet many requirements in metalation, transamination, and salt metathesis reactions, the knowledge of alkali metal amides is mainly limited to lithium amides for many reasons such as solubility in common organic solvents, commercial availability, NMR-active lithium isotopes, moderate reactivity, and the ease of crystallizing these derivatives.[1,2,18] The use of heavier alkali metals often leads to increased reactivity, enhanced ionicity of the A–N bond, and enhanced salt-like behavior, which includes poor solubility in common organic solvents. Despite the extensive use of potassium anilides in metathesis reactions, structural characterization is limited to a few examples, namely, $[(diox)KNPh_2]_\infty$,[19] $[(thf)_3KNPh_2]_2$,[20] $[(tmeda)_{1.5}KNPh_2]_\infty$,[21] and the separated ion pair [(18C6K)(NPh_2)] (18C6 = 18-crown-6).[22] More interest was paid to the bis(trimethylsilyl)amides of the heavier alkali metals, because the bulky $N(SiMe_3)_2$ ion ensures the formation of smaller aggregates and provides steric protection of the A–N bond, which lead to enhanced solubility and reduced sensitivity towards moisture and air and simplified preparation, handling, and manipulation. Despite the commercial availability of sodium and potassium bis(trimethylsilyl)amide and their use in many reactions, molecular structures are known for several sodium derivatives, whereas very few reports on potassium, rubidium, and cesium bis(trimethylsilyl)amides exist.[23] In all these alkali metal amides deaggregation can be achieved by Lewis bases depending on their denticity and donor strengths. The vastly growing importance of the organometallic chemistry of the heavier alkali metals[24] has led to a renewed interest in their amide chemistry, which can be seen in several recent investigations of Na(tmp),[25] $NaNPh_2$, and $KNPh_2$.[21]

Herein, light is shed on the influence of Lewis acidity (comparing the derivatives of sodium and potassium), the electronic and steric factors induced by the *N*-substituted anilide ions [N(Ph)R with R = Me, Ph, *i*Pr], and the neutral coligands (ethers, amines) on the solid-state structures, which focus on coordination number, degree of aggregation, and binding mode.

Results and Discussion

Preparation

The deprotonation of substituted anilines can be realized by a number of alkali metal compounds, such as alkyl, benzyl, and amido derivatives of alkali metals. All alkali metal anilides shown here were prepared by treating the underlying *N*-substituted aniline with commercially available $MN(SiMe_3)_2$ in toluene at room temperature, which yielded the corresponding anilides as fine white (sodium amides) or pale yellow solids (potassium amides) nearly quantitatively according to Equation (1). These alkali metal anilides are extremely sensitive towards moisture and air because of the lack of shielding coligands. An alternative route was chosen for NaN(Ph)*i*Pr, which involved deprotonation with $NaNH_2$ in toluene and proved to be advantageous, because gaseous ammonia evaporated to leave a pure compound. In contrast to this protocol, starting from $NaN(SiMe_3)_2$ afforded a suspension, which led to a challenging purification procedure to obtain the desired sodium anilide.

$$HN(Ph)R + A\{N(SiMe_3)_2\} \xrightarrow[-\,HN(SiMe_3)_2]{\text{toluene, r.t., 2 h}} AN(Ph)R \xrightarrow{+\,L} [(L)AN(Ph)R]_n \quad (1)$$

Compd.	A	R	L	Compd.	A	R	L
1	K	Ph	pmdta	**8**	K	*i*Pr	dme
2	K	*i*Pr	pmdta	**9**	Na	Ph	diox
3	Na	Ph	thf	**10**	Na	*i*Pr	diox
4	Na	*i*Pr	dme	**11**	K	Me	–
5	Na	Ph	pmdta	**12**	K	*i*Pr	thf
6	Na	*i*Pr	thf	**13**	K	*i*Pr	thf
7	Na	*i*Pr	tmeda	**14**	K	*i*Pr	dme

Molecular Structures

A dimeric unit with a central, in most cases planar, M_2N_2 core is the ubiquitous structural motif in alkali metal amide chemistry.[2] Whenever possible, alkali metal ions are coordinatively saturated by neutral Lewis bases (ethers or amines), which show an increasing tendency towards the heavier alkali metals by interactions between the alkali metal cations and the π-systems of phenyl groups. These coordination modes lead to three types of molecular structures: isolated dimers of the type $[(L)_mAN(Ph)R]_2$, dimers aggregated to polymeric strands by oligodentate coligands, and polymeric strands, layers, or 3D structures with bridging amido ions.

In centrosymmetric $[(pmdta)KNPh_2]_2$ (**1**, Figure 1) the potassium coordination polyhedron is best described as a distorted trigonal bipyramid with N1 and N3 in axial positions enclosing an angle with K1 of 166.4° as a consequence of small bite angles [N3–K1–N2 63.00(8)° and N3–K1–N4 62.1(1)°]. The central planar K_2N_2 ring is characterized by nearly equal K1–N1 distances of 282.1(2) and 283.7(3) pm and an N1–K1–N1A angle of 95.31(7)°. The C1–N1–C7 bond angle of 119.8(2)° hints towards sp^2 hybridization of N1. This larger angle reduces the steric hindrance between the phenyl groups. Because of the mainly ionic K1–N1 bonds, the necessity to form four covalent bonds and, hence, an sp^3 hybrid is reduced. Selected structural parameters are listed in Table 1 together with the data of the other anilide complexes discussed below.

Table 1. Selected bond lengths [pm] and angles [°] for **1**–**14** with some literature examples for comparison (D = donor, neutral coligand; X = centroid of phenyl ring).

(i) Molecular dimeric substituted alkali metal anilides								
Compound		M–N1	M–N1A	M–D1	M–D2	M–D3	M–N–M, N–M–N	N: angular sum
$[(pmdta)KN(Ph)_2]_2$	**1**	282.1(2)	283.7(3)	292.9(3)	281.3(3)	302.3(3)	84.69(7), 95.31(7)	348.6
$[(pmdta)KN(Ph)i Pr]_2$	**2**	279.6(1)	298.6(1)	303.2(2)	292.6 (2)	297.3(2)	89.39(4), 90.61(4)	360.0
$[(thf)_2NaN(Ph)_2]_2$	**3**	240.3(2)	247.8(2)	228.6(2)	230.8(2)		84.69, 95.31	357.3
$[(dme)NaN(Ph)i Pr]_2$	**4**	237.9(1)	251.3(1)	240.9(1)	235.7(1)		83.77(4), 96.23(4)	357.1
$[(pmdta)NaN(Ph)_2]_2$	**5**	248.8(2)	258.9(2)	274.7(2)	259.0(2)	267.3(2)	89.25(6), 90.75(6)	348.9
$[(thf)_2NaN(Ph)i Pr]_2$	**6**	242.0(2)	250.5(2)	234.7(2)	229.7(2)		81.06(7), 98.94(7)	348.3
$[(tmeda)NaN(Ph)i Pr]_2$	**7**	242.3(2)	248.7(2)	250.6(2)	247.8(2)		79.18(6), 100.82(6)	349.8
$[(dme)_2KN(Ph)i Pr]_2$	**8**	K1: 284.8(2)	284.8(2)	280.3(1),	289.6(1),		93.48(6)	336.6
		K2: 289.8(2)	289.8(2)	282.8(1)	294.6(2)		[85.59(6), 87.44(6)]	
$[(tmeda)NaN(Ph)_2]_2$	[21]	Na1: 242.2(2)	243.6(2)	246.6(2)	246.0(2)		81.74(7), 99.43(8)	
		Na2: 248.4(2)	246.6(2)	247.9(2)	249.8(2)		81.81(7), 96.96(7)	
$[(thf)_3KN(Ph)_2]_2$	[20]	279.5(2)	285.6(2)	272.6(2)	272.5(2)	270.9(2)		
(ii) Polymeric structures consisting of donor-bridged dimeric alkali metal anilides								
Compound		M–N1	M–N1A	M–D1	M–D2	M–D3	M–N–M, N–M–N	N: angular sum
$[\{(diox)_{1.33}NaN(Ph)_2\}_3]_\infty$	**9**	Na1: 241.6(2)	251.0(2),	248.6(2),	231.6(1),	241.4(2)	86.40(6), 89.00(6)	357.7 360.0 358.7
		Na2: 247.1(2)	249.4(2),	234.3(2),	233.8(2),		92.72(6), 91.83(6)	
		Na3: 235.9(2)	255.1(2)	232.9(2)	233.4(2)		86.90(6), 93.10(6)	
$[(diox)NaN(Ph)i Pr]_\infty$	**10**	239.0(3)	252.4(3)	233.1(3)	234.9(3)		81.43(9), 98.57(9)	356.3
$[(diox)_{1.5}KN(Ph)_2]_\infty$	[19]	279.0(1)	290.2(1)	266.6(1)	274.8(1)	275.2(1)		
$[(tmeda)_{1.5}KN(Ph)_2]_\infty$	[21]	282.3(2)	292.4(2)	287.1(2)	293.8(2)	331.4(2)	99.45(3), 80.55(3)	
(iii) Polymeric structures with intensive K–π-phenyl interactions as interconnecting principle								
$[\{KN(Ph)Me\}_3]_\infty$	**11**	K1: 275.9(4)	284.6(4)	M–X:	306.9 315.5	312.4		
		K2: 272.1(5)	278.8(4),		285.7			
			280.2(4)					
		K3: 285.0(4)	300.2(4)					
$[\{(thf)KN(Ph)i Pr\}_5]_\infty$	**12**	278.3(4)–	281.6(4)–	268.9(4)–	M–X 298.1			
		278.8(4)	284.5(4)	276.9(4)	(av.)			
$[\{(thf)_{0.5}KN(Ph)i Pr\}_2]_\infty$	**13**	K1: 285.5(2)	283.6(2)	286.4(2)	266.1(2)	M–Xb:	90.70(6), 89.30(6)	342.2 348.3
		K2: 270.1(2)			M–Xa: 285.6	283.4		
$[(dme)_{0.25}KN(Ph)i Pr]_\infty$	**14**	K1: 282.7(2)	286.0(2)	282.8(2)	273.4(2)	M–Xb:	88.86(6), 91.14(6)	340.7 347.7
		K2: 274.4(2)			M–Xa: 286.0	284.6		

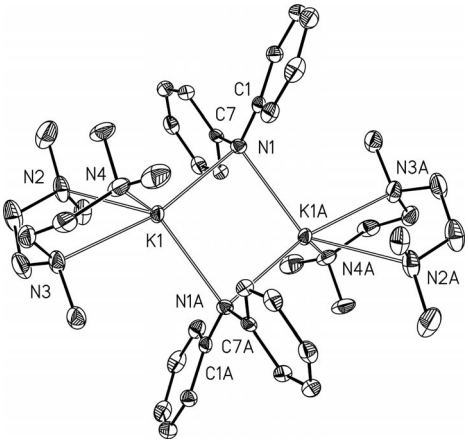

Figure 1. Molecular structure and numbering scheme of centrosymmetric **1**. Symmetry-related atoms (–*x* + 1, –*y* + 1, –*z* + 1) are marked with the letter "A". The ellipsoids represent a probability of 40%. H atoms are omitted for clarity. Selected bond lengths [pm] and angles [°]: K1–N1 282.1(2), K1–N1A 283.7(3), K1–N2 292.9(3), K1–N3 281.3(3), K1–N4 302.3(3), N1–C1 137.2(4), N1–C7 138.1(4), N1–K1–N1A 95.31(7); N2–K1–N3 63.00(8), N2–K1–N4 101.06(9), N3–K1–N4 62.13(10), C1–N1–C7 119.8(2).

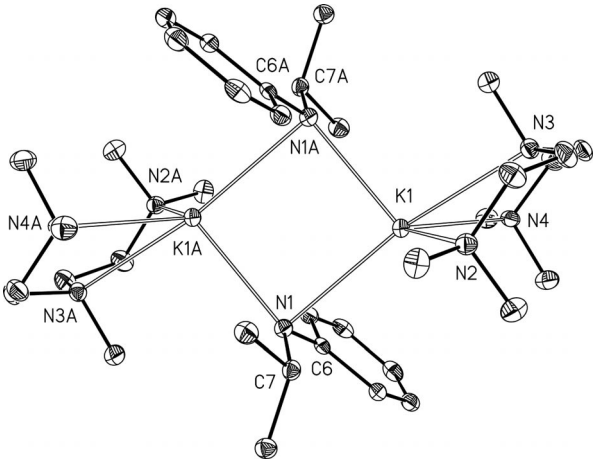

Figure 2. Molecular structure and numbering scheme of centrosymmetric **2**. Symmetry-related atoms (–*x* + 1, –*y* + 1, –*z* + 1) are marked with the letter "A". The ellipsoids represent a probability of 40%. H atoms are omitted for clarity. Selected bond lengths [pm] and angles [°]: K1–N1 298.6(2), K1–N1A 279.6(1), K1–N2 303.2(2), K1–N3 292.6(2), K1–N4 297.3(2), N1–C6 134.4(2), N1–C7 145.4(2), N1–K1–N1A 90.61(4); N2–K1–N3 60.28(4), N2–K1–N4 109.28(4), N3–K1–N4 61.01(4), C6–N1–C7 117.3(1).

Enhancement of the bulkiness of the anilido ion by substitution of one phenyl group of **1** by an isopropyl substituent yields $[(pmdta)KN(Ph)i Pr]_2$ (**2**), which has a different molecular structure to **1** (Figure 2). Although a comparable centrosymmetric dimeric molecule with a planar K1–N1

ring is observed in the solid state, there are notable differences. The K1–N1A and K1–N1 distances differ significantly with values of 279.6(1) and 298.6(1) pm, respectively. Again, the amido nitrogen atom [C6–N1–C7 117.3(1)°] can be regarded as sp^2-hybridized. Because of a larger s-orbital contribution between K1 and N1A this distance is 19 pm shorter than the K1–N1 bond to a nearly pure p orbital. This side-on coordination also leads to short K1–C6 contacts of only 303.7(2) pm. This description of the bonding situation is supported by the planarity of the K1A–N1–C6–C7 fragment with the sum of the angles of 359.97° at N1. In addition, the phenyl group shows a coplanar arrangement to this unit, which allows effective backdonation of negative charge from the amide functionality to the aryl group. This charge delocalization causes a shortening of the N1–C6 bond [134.4(2) pm], whereas in **1** values of 137.2(4) and 138.1(4) pm and a propeller-like orientation were observed. As expected, the N1–C7 bond [145.4(2) pm] to the alkyl group in **2** is much longer than that in **1**. The charge delocalization reduces the negative charge on N1 and, hence, the electrostatic attraction between the K^+ ion and the anilide, which is balanced by enhanced covalent bonding contributions.

Isolated molecules with central four-membered A_2N_2 rings were also found for many other sodium anilides such as $[(thf)_2NaNPh_2]_2$ (**3**, Figure S1), $[(dme)NaN(Ph)iPr]_2$ (**4**, Figure S2), $[(pmdta)NaN(Ph)H]_2$,[26] $[(pmdta)NaNPh_2]_2$ (**5**), $[(thf)_2NaN(Ph)iPr]_2$ (**6**, Figure S3), $[(tmeda)NaN(Ph)iPr]_2$ (**7**, Figure S4), $[(dme)_2KN(Ph)iPr]_2$ (**8**, Figure S5), $[(tmeda)NaNPh_2]_2$,[21] and $[(thf)_3KNPh_2]_2$.[20] The tilt of the bridging anilido ligand in **2** leads to significantly different K1–N1–C and K1A–N1–C angles. Another distortion is the twisting of the anilide ion, which leads to different A1–N1–C1 and A1–N1–C7 angles. This distortion was found for $[(pmdta)NaNPh_2]_2$ (**5**, Figure 3) with distal and proximal Na1A–N1–C angles of 121.3(1) and 107.9(1)° and Na1AA–N1–C angles of 109.3(1) and 103.7(1)°. In addition, different Na–N1 bond lengths of 248.8(2) and 258.9(2) pm were observed. In most cases, as observed for **5**, both types of distortion are more or less expressed depending on the bulkiness of the anilide and the denticity and steric demand of the neutral coligand. Additional molecular structures and numbering schemes are presented in the Supporting Information.

Polymeric structures based on the A_2N_2 core can be built with suitable bidentate bridging ligands, such as dioxane in $[(diox)_{1.33}NaNPh_2]_\infty$ (**9**, Figures S6 and S7), $[(diox)NaN(Ph)iPr]_\infty$ (**10**), and $[(diox)_{1.5}KNPh_2]_\infty$[12] and tmeda in $[(tmeda)_{1.5}KNPh_2]_\infty$.[14] Figure 4 shows the exemplary layer structure of **10**. The sodium anilide forms a four-membered ring with two different Na1–N1 and Na1–N1A bond lengths of 239.0(3) and 252.4(3) pm, respectively. The dimeric unit shows a similar tilt to that observed in **2**. The Na1–N1–C6–C7 unit is nearly planar with the sum of the angles at N1 of 356.3°. Two 1,4-dioxane molecules interconnect these Na_2N_2 rings, which leads to a layer structure with Na_2N_2 rings (oriented perpendicular to this layer) and tetracoordinate sodium atoms in distorted tetrahedral environments. Reduction of the anion size allows the coordination of three 1,4-dioxane molecules to one third of the sodium atoms, which are pentacoordinate. The increased coordination number leads to an elongation of the average Na–O bonds from 234 to 241 pm, whereas the Na–N distances exhibit comparable values of 241.6(2) and 251.0(2) pm.

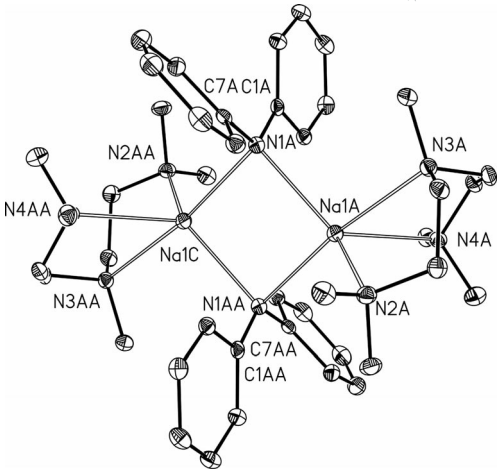

Figure 3. Molecular structure and numbering scheme of centrosymmetric **5**. Only molecule A of the two crystallographically independent molecules is shown. Symmetry-related N and C atoms ($-x + 1$, $-y + 1$, $-z + 1$) are marked with the letter "A", Na1C is generated by the same symmetry operation. The ellipsoids represent a probability of 40%. H atoms are omitted for clarity. Selected bond lengths [pm] and angles [°]: Na1A–N1A 248.8(2), Na1A–N1AA 258.9(2), Na1A–N2A 274.7(2), Na1A–N3A 259.0(2), Na1A–N4A 267.3(2), N1A–C1A 137.9(3), N1A–C7A 140.0(3); N1A–Na1A–N1AA 90.75(6), N2A–Na1A–N3A 70.13(6), N2A–Na1–N4A 105.44(6), N3A–Na1A–N4A 70.78(6), C1A–N1A–C7A 119.6(2).

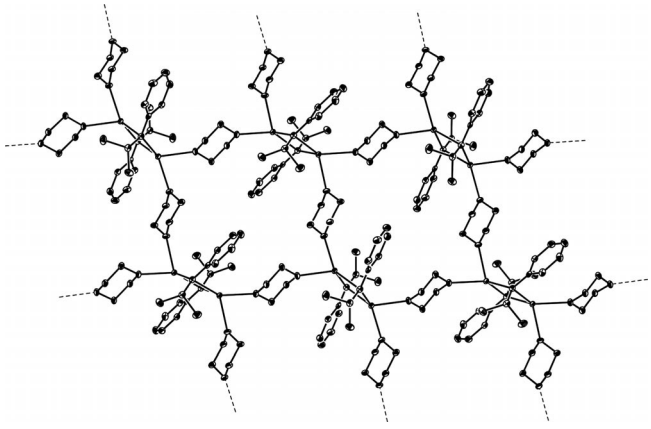

Figure 4. Representation of the layer structure of **10**. The ellipsoids represent a probability of 40%. H atoms are omitted for clarity. The centrosymmetric Na_2N_2 rings are oriented perpendicular to the layer and bridged by 1,4-dioxane molecules. Selected bond lengths [pm] and angles [°] for a dinuclear unit: Na1–N1 239.0(3), Na1–N1A 252.4(3), Na1–O1 233.1(3), Na1–O2 234.9(3), N1–$C6_{Ph}$ 136.0(4), N1–$C7_{iPr}$ 145.8(5); N1–Na1–N1A 98.57(9), O1–Na1–O2 81.31(9), C6–N1–C7 116.0(3).

Whereas the hard sodium ion prefers hard Lewis donors such as ethers and amines, the softer potassium ion binds to soft arene π-systems. Thus, substituted anilides, which are comparable to their isoelectronic benzyl congeners,[27] tend to build polymeric structures by bridging up to four soft alkali metal centers (Figure 5) both by metal binding to the amido functionality and to the arene π-system. This can be observed in $[KN(Ph)Me]_\infty$ (**11**), which was obtained without coligands from a saturated THF solution. The framework of **11** is built of three crystallographically independent potassium *N*-methylanilides. The central units of this structure are two twelve-membered rings that consist of $(K2–N1B)_6$ and $(K3–N1C)_6$, which are interconnected by K1–N1A bridges (Figures 6 and S10). The K–N distances vary within a rather large range of 272.1(5)–300.2(4) pm. The K–C distances also vary within a large range with the shortest K–C bond length of 305.0(5) pm with a cut off at 330 pm.[24]

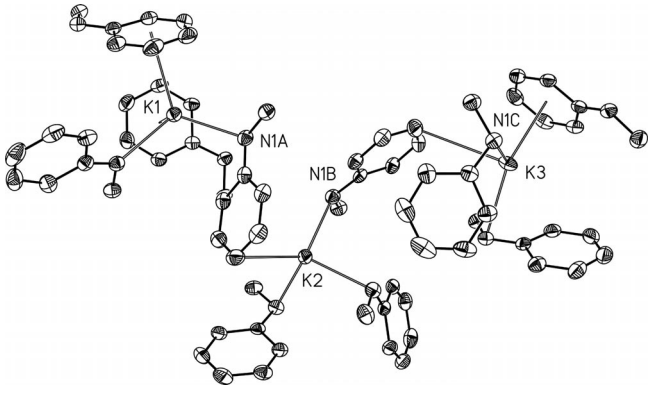

Figure 5. Representation of the coordination spheres of the potassium ions in **11**. K1 binds to two amides and interacts with the π-systems of two phenyl groups, K2 binds to three amides and shows a close contact to a *para*-CH unit of a neighboring phenyl group, K3 binds to two amides as well as to two phenyl groups with η^1- and η^6-coordination modes.

Part of the polymeric helical structure of $[\{(thf)KN(Ph)iPr\}_5]_\infty$ (**12**) and the numbering scheme are displayed in Figure 7. In this structure five crystallographically independent {(thf)KN(Ph)*i*Pr} units are observed with very similar coordination spheres for all of the potassium ions. The K^+ ions are coordinated by two bridging nitrogen atoms with K–N distances in the range of 278.3(4)–284.5(4) pm. Obtuse K–N–K angles [98.47(13)–105.15(13)°] differ within a rather narrow range, which indicates comparable alkali metal environments. Coordinative saturation to give distorted tetrahedra is ensured by thf molecules with K–O distances ranging from 268.9(4)–276.9(4) pm and by η^6-phenyl interactions (average K–centroid distance 298.1 pm). Because of the enhanced steric demand of the isopropyl group compared to the methyl group, the maximum bridging capacity of one anilido ligand decreases from four to three potassium atoms.

Reduction of the thf content by half essentially leads to dimers of $[(thf)KN(Ph)iPr]_2$ with four-membered K_2N_2 rings. Another ether-free {KN(Ph)*i*Pr} unit binds to this

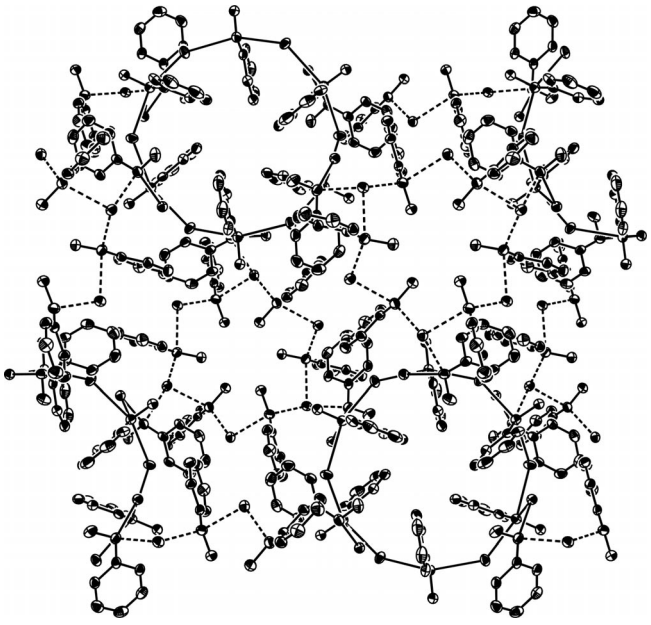

Figure 6. Packing of **11** in the solid state. The ellipsoids represent a probability of 40%. H atoms are omitted for clarity. Only K–N bonds are displayed, and interactions with neighboring phenyl groups are not shown. The two different types of twelve-membered K_6N_6 rings, which are distinguished by solid and dashed lines, are visualized in this representation.

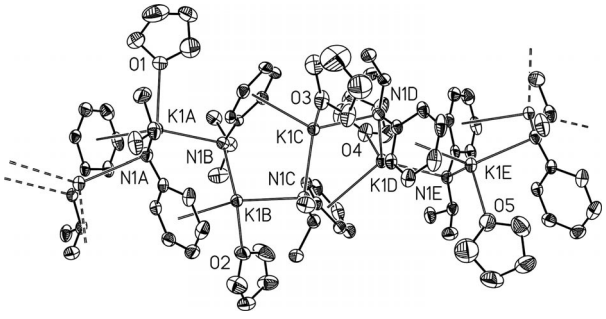

Figure 7. Part of the polymeric helical structure and numbering scheme of **12**. The ellipsoids represent a probability of 40%. H atoms are omitted for clarity. The potassium ions show short contacts to the soft π-systems of the phenyl groups in addition to K–N bonds.

dimer through a bridging nitrogen atom and a bridging η^6-bound phenyl group. Figure 8 shows a representative section of the chain structure and the numbering scheme for $[\{(thf)_{0.5}KN(Ph)iPr\}_2]_\infty$ (**13**). The anilide shows a very similar coordination mode to that in **12**: a nitrogen atom bridges to two metal ions, and the phenyl ring interconnects a third. The two crystallographically independent potassium ions exhibit significantly different coordination environments. K1 is coordinated in a distorted tetrahedron by three amide nitrogen atoms (average K–N distance 285.2 pm) and one thf molecule [K1–O1 266.1(2) pm], but no short contacts to carbon atoms are observed. If a η^6-phenyl interaction is regarded as one occupied coordination site, K2 is coordinated in a nearly trigonal-planar manner (sum of the

angles at K2 of 359.0°) with average distances of 284.5 pm to the phenyl centroids and a very short K2–N2 distance of 270.1(2) pm.

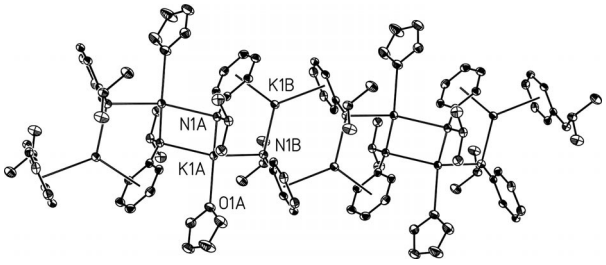

Figure 8. Part of the chain structure and numbering scheme of **13**. The ellipsoids represent a probability of 40%. H atoms are omitted for clarity. The characteristic centrosymmetric dimers with K_2N_2 rings are interconnected by {KN(Ph)*i*Pr} units, in which the potassium ions interact with the π-systems of the phenyl groups.

Replacement of the thf ligand by half a dme molecule results in isostructural $[(dme)_{0.25}KN(Ph)iPr]_\infty$ (**14**). Single chains are interconnected by bridging dme molecules to give a layer structure with parameters comparable to those of **13** (Table 1). A part of this structure is displayed in Figure 9. As seen for the thf adduct, the dme adduct was also obtained as dme-rich $[(dme)_2KN(Ph)iPr]_2$ (**8**), which is the only derivative with potassium ions coordinated by six heteroatom-based Lewis bases in this work. Remarkably, **14** crystallised from a DME solution, whereas **8** precipitated from a DME-containing toluene/pentane mixture.

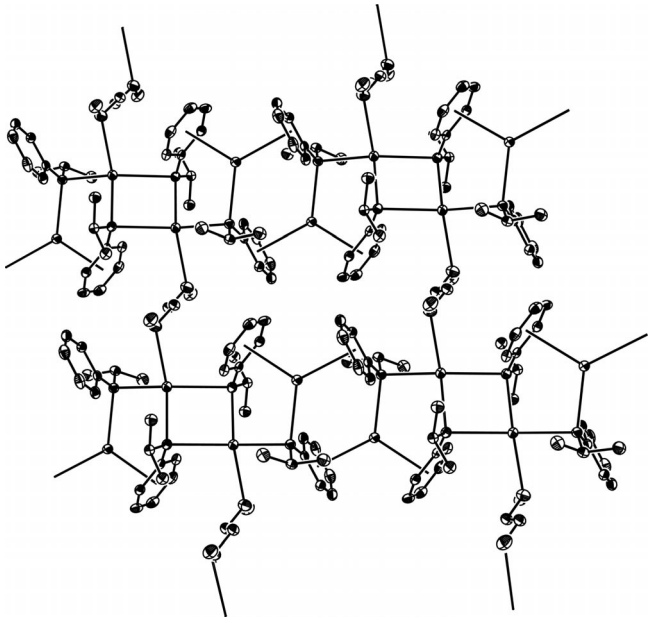

Figure 9. Layer structure of **14**. The ellipsoids represent a probability of 40%. H atoms are omitted for clarity. This layer structure is built by the chains shown in Figure 8, which are interconnected by bridging dme molecules.

Solution Studies

The ^1H and $^{13}C\{^1H\}$ NMR spectroscopic data of the phenyl groups for all compounds are listed in Tables 2 and 3, respectively, which includes the amines for comparison. All experiments were carried out in $[D_8]$THF solutions at 300 K. Notably, the *ipso* and *para* carbon atom signals in the $^{13}C\{^1H\}$ NMR spectra are often very broad (Table 3), which probably indicates high mobility and fast ligand exchange reactions.

Table 2. ^1H NMR spectroscopic data (chemical shifts) [ppm] of the phenyl groups in **1**–**14**; spectra were acquired at 200.13 MHz at 300 K in $[D_8]$THF.

Compound		Coligand	*o*-C*H*	*m*-C*H*	*p*-C*H*
HN(Ph)Me			6.56	7.10	6.58
K	**11**	$[D_8]$THF	6.10	6.78	5.83
$HNPh_2$			7.04	7.16	6.78
Na	**3**	thf	6.83–6.85		6.17
	9	diox	6.84–6.96		6.31
	5	pmdta	6.92–7.09		6.56
K	[20]	thf	6.85–6.87		6.15
	[19]	diox	6.85–6.90		6.16
	[21]	tmeda	6.84	6.84	6.14
	1	pmdta	6.87–6.90		6.21
HN(Ph)*i*Pr			6.53	7.04	6.52
Na	**6**	thf	6.30	6.82	5.95
	4	dme	6.15	6.70	5.72
	10	diox	6.13	6.70	5.73
	7	tmeda	6.16	6.70	5.72
K		$[D_8]$THF	6.27	6.84	6.04
	14	dme	6.27	6.84	6.04
	2	pmdta	6.13	6.74	5.76

Table 3. ^{13}C NMR spectroscopic data (chemical shifts) [ppm] of the phenyl groups for **1**–**14**; spectra were acquired at 50.33 MHz at 300 K in $[D_8]$THF.

Compound		Coligand	*i*-C*H*	*o*-C*H*	*m*-C*H*	*p*-C*H*
HN(Ph)Me			151.0	112.7	129.6	116.8
K	**11**	$[D_8]$THF	160.9	111.2	128.8	106.8
$HNPh_2$			145.0	118.2	129.7	120.8
Na	**3**	thf	157.8	118.6	129.4	113.5
	9	diox	155.0	118.3	129.3	114.6
	5	pmdta	149.3	118.0	129.5	117.8
K	[13]	thf	158.5	118.0	129.7	112.1
	[12]	diox	158.3	118.0	129.7	112.3
	[14]	tmeda	158.1	118.2	129.7	112.6
	1	pmdta	156.8	118.0	129.6	113.1
HN(Ph)*i*Pr			149.0	113.4	129.5	116.5
Na	**6**	thf	158.6	112.6	129.7	108.6
	4	dme	158.6	112.2	129.7	105.6
	10	diox	158.7	112.4	129.6	105.9
	7	tmeda	[a]	112.3	129.7	105.4
K		$[D_8]$THF	154.5	112.6	129.8	110.6
	14	dme	154.5	112.5	129.7	110.4
	2	pmdta	158.7	111.9	130.0	106.3

[a] Signal shift could not be identified due to signal broadness.

Phenylamides (anilides) and benzyl anions are isoelectronic, and they are expected to exert a similar influence on the negative charge delocalization on the NMR parameters.[28] The degree of charge delocalization strongly de-

pends on the hybridization of the amido nitrogen atom: the negative charge is mainly located on sp^3-hybridized N atoms, whereas an effective charge backdonation is realized with sp^2-hybridized amido functionalities. In agreement with this concept, the $\delta(^1H)$ values of the *para*-CH fragments of the amides show significant high-field shifts due to backdonation of negative charge from the amido functionalities compared to the free amines. A similar trend, although less pronounced, is observed for the *ortho*- and *meta*-CH moieties. For the $^{13}C\{^1H\}$ chemical shifts, a similar tendency was found for the *ipso*-carbon atoms. However, the *ortho*-C signals experience a strong low-field shift of roughly 10 ppm compared to those of the free amine, whereas there is only a marginal influence on the $\delta(^{13}C\{^1H\})$ values of the *meta*-CH units. The differences between the sodium and potassium derivatives are small, which suggests largely ionic bonds between the anilide and the alkali metal ions. Nevertheless, the trends described above are a little more obvious for the potassium derivative when comparing derivatives with the same coligands. The diphenylamides bound to sodium show $^{13}C\{^1H\}$ NMR chemical shifts for the *para*-carbon atom of δ = 113.5, 114.6, and 117.8 ppm with thf, diox, and pmdta coligands, whereas for the potassium derivatives, values of δ = 112.1, 112.3, and 113.1 ppm are observed.

Summary and Conclusion

Substituted alkali metal anilides are accessible from the transamination of the alkali metal bis(trimethylsilyl)amides. The molecular structures of these derivatives depend on the presence and donor strength of the neutral coligands (ethers and amines) as well as the steric demand of these coligands and the substituted anilide ions. The central motif in the series of sodium anilides is a four-membered Na_2N_2 ring with the sodium ions coordinatively saturated by coligands, with the exception of solvent-free trimeric $NaN(SiMe_3)_2$.[23d,23e] A sufficient supply of Lewis bases yields dinuclear molecules as found in $[(thf)_2NaNPh_2]_2$ (**3**), $[(dme)NaN(Ph)iPr]_2$ (**4**), $[(pmdta)NaNPh_2]_2$ (**5**), $[(thf)_2NaN(Ph)iPr]_2$ (**6**), and $[(tmeda)NaN(Ph)iPr]_2$ (**7**). The use of bidentate Lewis bases that can act as chelating ligands leads to the formation of layer structures as observed for the 1,4-dioxane complexes $[(diox)_{1.33}NaNPh_2]_\infty$ (**9**) and $[(diox)NaN(Ph)iPr]_\infty$ (**10**). In these structures the Na_2N_2 rings are oriented perpendicular to the layer.

Much more complex coordination behavior was observed for the homologous potassium derivatives. The potassium ion adopts an intermediate position between hard and soft Lewis acids. Therefore, similar structures as those found for the sodium complexes can be expected, but the π-systems of the arenes can also act as soft Lewis bases. Therefore, characteristic structural features, such as the K_2N_2 ring, can be found in the dinuclear molecules $[(pmdta)KNPh_2]_2$ (**1**), $[(pmdta)KN(Ph)iPr]_2$ (**2**), and $[(dme)_2KN(Ph)iPr]_2$ (**8**). The missing chelating effect of monodentate Lewis-basic coligands allows the reduction of the number of ether and amine bases, which leads to vacant coordination sites. Because of this arrangement, further KN(Ph)*i*Pr moieties are attached to two opposite sides of the molecule with the potassium ion binding to the π-system of the phenyl group. This coordination behavior gives a strand structure of the type $[\{(thf)KN(Ph)iPr\}_2{\cdot}2KN(Ph)iPr]$ (**13**) with the two K^+ ions being part of a four-membered K_2N_2 ring, and the other two K^+ ions bound to one amido functionality and side-on to two phenyl rings. Substitution of the thf coligand by a bidentate dme molecule leads to the connection of the $[KN(Ph)iPr]_\infty$ strands to form a layer structure: $[(dme)_{0.25}KN(Ph)iPr]_\infty$ (**14**). Again, only half of the potassium ions bind to neutral coligands. If all of the potassium ions carry a neutral Lewis donor such as thf, as in $[(thf)KN(Ph)iPr]_\infty$ (**12**), the central K_2N_2 ring is broken up, and the thf molecules, amido ions, and π-systems of the phenyl groups act as comparable donors with similar affinities for K^+. The absence of neutral coligands and the reduction of the bulk of the amido ions leads to the formation of a 3D framework as observed in $[KN(Ph)Me]_\infty$ (**11**).

All the alkali metal anilides described here exhibit significant solubility in THF and less in aromatic hydrocarbons. This finding suggests a breakdown of the polymeric and oligomeric structures in THF, and therefore the solutions contain smaller units. Dinuclear compounds with Na_2N_2 rings can be expected for the sodium derivatives. Similar behavior can also be expected for the homologous potassium derivatives on the basis of their comparable solubilities. The NMR parameters suggest a mainly ionic bonding situation; however, the ionic character of these substituted alkali metal anilides is expected to be a little more expressed in the potassium derivatives.

Experimental Section

General Remarks: All manipulations were carried out under argon by using standard Schlenk techniques. Solvents were dried according to common procedures and distilled under argon. Deuterated solvents were dried with sodium, degassed, and saturated with argon. The ^1H and $^{13}C\{^1H\}$ NMR spectra were obtained with Bruker AC 400 MHz or Bruker 200 MHz spectrometers.

General Procedure for the Syntheses of AN(Ph)R with $AN(SiMe_3)_2$ (A = Na, K): $AN(SiMe_3)_2$ (10 mmol) was dissolved in toluene (20 mL). To this solution HN(Ph)R (10.5 mmol) was added dropwise at room temperature to obtain a precipitate of AN(Ph)R. After stirring for 2 h, the product was collected on a frit and washed twice with toluene (3 mL) and pentane (3 mL). The crude product was dried in vacuo to yield solvent-free alkali metal anilides with isolated yields of 97–99%. Due to the fact that the formation of adducts with ethers and amine bases is quantitative, yields are not given below. In order to obtain crystalline material, the amorphous alkali metal anilides were dissolved in the desired solvent with heating. Cooling of these solutions to room temperature or –20 °C gave crystalline material suitable for single-crystal diffraction studies. Other protocols for recrystallization, if used, are mentioned below.

KN(Ph)*i*Pr: ^{1}H NMR ([D$_8$]THF): δ = 6.84 (dd, $^3J_{H,H}$ = 7.2 + 8.4 Hz, 2 H, *m*-H), 6.27 (d, $^3J_{H,H}$ = 8.0 Hz, 2 H, *o*-H), 6.04 (t, $^3J_{H,H}$ = 6.4 Hz, 1 H, *p*-H), 3.47 (sept, $^3J_{H,H}$ = 6.2 Hz, 1 H, C*H*), 1.11 (d, $^3J_{H,H}$ = 6.2 Hz, 6 H, CH_3) ppm. ^{13}C{^{1}H} NMR ([D$_8$]THF): δ = 154.5 (*i*-C), 129.8 (*m*-C), 112.6 (*o*-C), 110.6 (*p*-C), 45.9 (*C*H), 23.9 (*C*H$_3$) ppm.

[(pmdta)KNPh$_2$]$_2$ (1): ^{1}H NMR ([D$_8$]THF): δ = 6.90–6.87 (m, 16 H, *o*-H + *m*-H), 6.28–6.17 (m, $^3J_{H,H}$ = 7.0 Hz, 4 H, *p*-H), 2.45–2.26 (m, 16 H, CH_2, pmdta), 2.18 (s, 6 H, CH_3, pmdta), 2.14 (s, 24 H, CH$_3$, pmdta) ppm. ^{13}C{^{1}H} NMR ([D$_8$]THF): δ = 156.8 (*i*-C), 129.6 (*m*-C), 118.0 (*o*-C), 113.1 (*p*-C), 58.7 and 57.2 (*C*H$_2$, pmdta), 46.1 (8 *C*H$_3$, pmdta), 43.1 (2 *C*H$_3$, pmdta) ppm.

[(pmdta)KN(Ph)*i*Pr]$_2$ (2): Crystals were obtained by dissolving a totally dry sample of K$_2$Ca[N(Ph)*i*Pr]$_4$ in PMTDA (2 mL) with heating and subsequent slow cooling to room temperature. ^{1}H NMR ([D$_8$]THF): δ = 6.74 (dd, $^3J_{H,H}$ = 7.4 + 8.2 Hz, 4 H, *m*-H), 6.13 (d, $^3J_{H,H}$ = 8.2 Hz, 4 H, *o*-H), 5.76 (t, $^3J_{H,H}$ = 7.0 Hz, 4 H, *p*-H), 3.39 (sept, $^3J_{H,H}$ = 6.2 Hz, 1 H, C*H*), 2.46–2.26 (m, 16 H, CH_2, pmdta), 2.19 (s, 6 H, CH_3, pmdta), 2.15 (s, 24 H, CH$_3$, pmdta), 1.09 (d, 6 H, $^3J_{H,H}$ = 6.2 Hz, CH_3) ppm. ^{13}C{^{1}H} NMR ([D$_8$]THF): δ 158.7 (*i*-C), 130.0 (*m*-C), 111.2 (*o*-C), 106.3 (*p*-C), 58.8 and 57.3 (*C*H$_2$, pmdta), 47.0 (*C*H), 46.1 (8 *C*H$_3$, pmdta), 43.2 (2 *C*H$_3$, pmdta), 24.6 (*C*H$_3$) ppm.

[(thf)$_2$NaNPh$_2$]$_2$ (3): A concentrated THF solution (1 mL) of NaNPh$_2$ (1.3 g of amide in 4 mL of THF) was cooled to –20 °C. Crystals of **3** precipitated within 12 h, which were suitable for single-crystal X-ray structure analysis. ^{1}H NMR ([D$_8$]THF): δ = 6.83–6.85 (m, 16 H, *o*-H + *m*-H), 6.17–6.27 (m, 4 H, *p*-H), 3.60 (thf), 1.77 (thf) ppm. ^{13}C{^{1}H} NMR ([D$_8$]THF): δ = 157.8 (*i*-C), 129.4 (*m*-C), 118.6 (*o*-C), 113.5 (*p*-C), 68.1 (thf), 26.3 (thf) ppm.

[(dme)NaN(Ph)*i*Pr]$_2$ (4): ^{1}H NMR ([D$_8$]THF): δ = 6.70 (dd, $^3J_{H,H}$ = 7.0 + 8.6 Hz, 8 H, *m*-H), 6.15 (d, $^3J_{H,H}$ = 8.2 Hz, 8 H, *o*-H), 5.72 (t, $^3J_{H,H}$ = 6.4 Hz, 2 H, *p*-H), 3.43 (CH_2, dme), 3.40 (sept, $^3J_{H,H}$ = 6.0 Hz, 2 H, C*H*), 3.27 (CH_3, dme), 1.10 (d, $^3J_{H,H}$ = 6.2 Hz, 12 H, CH_3) ppm. ^{13}C{^{1}H} NMR ([D$_8$]THF): δ = 158.6 (*i*-C), 129.7 (*m*-C), 112.2 (*o*-C), 105.6 (*p*-C), 72.6 (*C*H$_2$, dme), 58.8 (*C*H$_3$, dme), 47.5 (*C*H), 25.3 (*C*H$_3$) ppm.

[(pmdta)NaNPh$_2$]$_2$ (5): ^{1}H NMR ([D$_8$]THF): δ = 6.92–7.09 (m, 16 H, *o*-H + *m*-H), 6.56 (dd, $^3J_{H,H}$ = 7.0 Hz, 4 H, *p*-H), 2.48–2.27 (m, 16 H, CH_2, pmdta), 2.20 (s, 6 H, CH_3, pmdta), 2.15 (s, 24 H, CH$_3$, pmdta) ppm. ^{13}C{^{1}H} NMR ([D$_8$]THF): δ = 149.3 (*i*-C), 129.5 (*m*-C), 118.0 (*o*-C), 117.8 (*p*-C), 58.7 and 57.3 (*C*H$_2$, pmdta), 46.1 (8 *C*H$_3$, pmdta), 43.2 (2 *C*H$_3$, pmdta) ppm.

[(thf)$_2$NaN(Ph)*i*Pr]$_2$ (6): ^{1}H NMR ([D$_8$]THF): δ = 6.82 (dd, $^3J_{H,H}$ = 7.4 + 8.2 Hz, 4 H, *m*-H), 6.30 (d, $^3J_{H,H}$ = 8.0 Hz, 4 H, *o*-H), 5.95 (t, $^3J_{H,H}$ = 6.6 Hz, 2 H, *p*-H), 3.62 (thf), 3.43 (sept, $^3J_{H,H}$ = 6.0 Hz, 2 H, C*H*), 1.78 (thf), 1.11 (d, $^3J_{H,H}$ = 6.2 Hz, 12 H, CH_3) ppm. ^{13}C{^{1}H} NMR ([D$_8$]THF): δ = 158.6 (*i*-C), 129.7 (*m*-C), 112.6 (*o*-C), 108.6 (*p*-C), 68.1 (thf), 46.8 (*C*H), 26.3 (thf), 24.8 (*C*H$_3$) ppm.

[(tmeda)NaN(Ph)*i*Pr]$_2$ (7): ^{1}H NMR ([D$_8$]THF): δ = 6.70 (dd, $^3J_{H,H}$ = 7.0 + 8.6 Hz, 8 H, *m*-H), 6.16 (d, $^3J_{H,H}$ = 8.2 Hz, 8 H, *o*-H), 5.72 (t, $^3J_{H,H}$ = 6.4 Hz, 2 H, *p*-H), 3.40 (sept, $^3J_{H,H}$ = 6.2 Hz, 2 H, C*H*), 2.30 (tmeda, CH_2), 2.14 (CH_3, tmeda), 1.11 (d, $^3J_{H,H}$ = 6.0 Hz, 12 H, CH_3) ppm. ^{13}C{^{1}H} NMR ([D$_8$]THF): δ = (*i*-C, not observed) 129.7 (*m*-C), 112.3 (*o*-C, br.), 105.4 (*p*-C, br.), 58.7 (*C*H$_2$, tmeda), 47.6 (*C*H), 46.0 (*C*H$_3$, tmeda), 25.4 (*C*H$_3$) ppm.

[(dme)$_2$KN(Ph)*i*Pr]$_2$ (8): Only very few slow-growing crystals were obtained at –20 °C from a toluene/pentane/DME solution that contained a 2:1 stoichiometric ratio of K/Ca anilide.

[(diox)$_4$Na$_3$(NPh$_2$)$_3$ (diox)]$_\infty$ (9): ^{1}H NMR ([D$_8$]THF): δ = 6.84–6.96 (m, 24 H, *o*-H and *m*-H), 6.27–6.35 (m, 6 H, *p*-H), 3.56 (diox) ppm. ^{13}C{^{1}H} NMR ([D$_8$]THF): δ = 155.0 (*i*-C), 129.3 (*m*-C), 118.3 (*o*-C), 114.6 (*p*-C), 67.7 (diox) ppm.

[(diox)NaN(Ph)*i*Pr (THF)]$_\infty$ (10): ^{1}H NMR ([D$_8$]THF): δ = 6.70 (dd, $^3J_{H,H}$ = 7.4 and 7.8 Hz, 8 H, *m*-H), 6.13 (d, $^3J_{H,H}$ = 8.0 Hz, 8 H, *o*-H), 5.73 (br., 2 H, *p*-H), 3.57 (CH_2, diox), 3.40 (sept, $^3J_{H,H}$ = 6.2 Hz, 2 H, C*H*), 1.09 (d, $^3J_{H,H}$ = 6.2 Hz, 12 H, CH_3) ppm. ^{13}C{^{1}H} NMR ([D$_8$]THF): δ = 158.7 (*i*-C), 129.6 (*m*-C), 112.4 (*o*-C), 105.9 (*p*-C), 68.1 (thf), 67.7 (*C*H$_2$, diox), 47.3 (*C*H), 26.2 (thf), 25.2 (*C*H$_3$) ppm.

[{KN(Ph)Me}$_3$]$_\infty$ (11): The amorphous KN(Ph)Me obtained from applying the general procedure was dissolved in THF. This concentrated solution was stored at –20 °C to generate crystalline **11**, which did not contain solvent. ^{1}H NMR ([D$_8$]THF): δ = 6.78 (dd, $^3J_{H,H}$ = 7.8 Hz, 2 H, *m*-H), 6.10 (d, $^3J_{H,H}$ = 7.8 Hz, 2 H, *o*-H), 5.83 (t, $^3J_{H,H}$ = 7.0 Hz, 1 H, *p*-H), 2.76 (s, 3 H, CH$_3$) ppm. ^{13}C{^{1}H} NMR ([D$_8$]THF): δ = 160.9 (*i*-C), 128.8 (*m*-C), 111.2 (*o*-C), 106.8 (*p*-C), 36.2 (CH$_3$) ppm.

[{(thf)KN(Ph)*i*Pr}$_5$(THF)$_2$]$_\infty$ (12): (a) KN(Ph)*i*Pr dissolved readily by warming in THF. Slow cooling to room temperature afforded crystalline needles of **12** and a solution that contained KN(Ph)*i*Pr (0.34 mol L^{-1}). (b) Compound **12** was also obtained from a THF solution that contained a 2:1 stoichiometry of K/Sr anilide.

[(thf)$_{0.5}$K{*N*(Ph)*i*Pr}]$_\infty$ (13): Small, slow-growing crystals of **13** precipitated from a THF-containing toluene/pentane (1:1) solution of KN(Ph)*i*Pr at –20 °C within 4 weeks.

[(dme)$_{0.25}$K{*N*(Ph)*i*Pr}]$_\infty$ (14): (a) Crystals suitable for XRD were initially obtained from a DME solution of K$_2$Ca[N(Ph)*i*Pr]$_4$. (b) Compound **14** was also isolated from a saturated THF solution of K{N(Ph)*i*Pr} (1.5 mL), which was dried in vacuo and redissolved in DME (2 mL). Reducion of the volume by about half yielded fast-growing crystals, which were used for NMR spectroscopy. The DME content was confirmed by NMR spectroscopy. ^{1}H NMR ([D$_8$]THF): δ = 6.84 (dd, $^3J_{H,H}$ = 8.4 + 7.0 Hz, 2 H, *m*-H), 6.27 (d, $^3J_{H,H}$ = 8.0 Hz, 2 H, *o*-H), 6.04 (t, $^3J_{H,H}$ = 7.0 Hz, 1 H, *p*-H), 3.47 (sept, $^3J_{H,H}$ = 6.2 Hz, 1 H, C*H*), 3.43 (ca. 1.1 H-equiv., CH_2, dme), 3.27 (ca. 1.9 H-equiv., CH_3, dme), 1.11 (d, $^3J_{H,H}$ = 6.4 Hz, 6 H, CH_3) ppm. ^{13}C{^{1}H} NMR ([D$_8$]THF): δ = 154.5 (*i*-C), 129.7 (*m*-C), 112.5 (*o*-C), 110.4 (*p*-C), 72.6 (*C*H$_2$, dme), 58.8 (*C*H$_3$, dme), 45.8 (*C*H), 23.9 (*C*H$_3$) ppm.

Structure Determination: The intensity data for the compounds were collected with a Nonius KappaCCD diffractometer by using graphite-monochromated Mo-K_α radiation. Data were corrected for Lorentz and polarization effects but not for absorption effects.[29,30] The structures were solved by direct methods (SHELXS[31]) and refined by full-matrix least-squares techniques against F_o^2 (SHELXL-97[31]). The hydrogen atoms in **2** and **4** were located by difference Fourier synthesis and refined isotropically. The other hydrogen atoms were included at calculated positions with fixed thermal parameters. Disorder in the ethylene bridge of a dme ligand was observed in **8**. The corresponding carbon atoms were refined freely with isotropic thermal parameters. All other non-hydrogen atoms were refined anisotropically.[31] The quality of the data obtained from **12** was poor and, as such, we only publish conformation of the molecule and the crystallographic data and will not deposit the data in the Cambridge Crystallographic Data Centre. Crystallographic data as well as structure solution and refinement details are summarized in Tables 4, 5, and 6. XP (SIEMENS Analytical X-ray Instruments, Inc.) was used to generate structure representations. CCDC-840059 (for **1**), -840060 (for **2**), -840061 (for **3**), -840062 (for **4**), -840063 (for **5**), -840064 (for **6**), -840065 (for **7**), -840066 (for **8**), -840067 (for **9**), -840068 (for

Table 4. Crystal data and refinement details for the X-ray structure determinations of **1**–**6**.

Compound	**1**	**2**	**3**	**4**	**5**	**6**
Empirical formula	$C_{42}H_{64}K_2N_8$	$C_{36}H_{70}K_2N_8$	$C_{40}H_{52}N_2Na_2O_4$	$C_{26}H_{44}N_2Na_2O_4$	$C_{42}H_{66}N_8Na_2$	$C_{34}H_{56}N_2Na_2O_4$
Formula mass [g mol^{-1}]	759.21	693.20	670.82	494.61	729.01	602.79
T [K]	–140(2)	–140(2)	–140(2)	–140(2)	–140(2)	–140(2)
Crystal system	triclinic	triclinic	triclinic	monoclinic	triclinic	triclinic
Space group	$P\bar{1}$	$P\bar{1}$	$P\bar{1}$	$P2_1/n$	$P\bar{1}$	$P\bar{1}$
a [Å]	10.3172(7)	10.4926(7)	8.4919(4)	8.9458(3)	10.7551(5)	9.2939(9)
b [Å]	10.9602(8)	10.5338(7)	10.9491(4)	16.7727(9)	11.5469(4)	9.7631(8)
c [Å]	11.0041(8)	11.1065(5)	21.0380(9)	9.8707(5)	17.2377(7)	10.8542(11)
α [°]	65.345(3)	78.955(3)	99.581(2)	90	88.145(2)	78.633(6)
β [°]	76.419(3)	62.761(3)	95.814(2)	107.439(3)	83.166(2)	70.024(6)
γ [°]	84.499(3)	67.445(2)	101.921(3)	90	80.085(2)	69.799(6)
V [Å^3]	1099.27(14)	1007.76(11)	1868.45(14)	1412.98(11)	2093.61(15)	865.19(14)
Z	1	1	2	2	2	1
ρ [g cm^{-3}]	1.147	1.142	1.192	1.163	1.156	1.157
μ [mm^{-1}]	2.53	2.69	0.96	1.03	0.87	0.96
Measured data	7795	7370	13588	9816	14458	4867
Data with $I > 2\sigma(I)$	3154	3186	5053	2020	5289	3025
Unique data (R_{int})	4981/0.0403	4587/0.0368	8434/0.0403	3233/0.0726	9487/0.0513	3645/0.0276
wR_2 (all data, on F^2)[a]	0.1887	0.1023	0.1317	0.0996	0.1399	0.1872
R_1 [$I > 2\sigma(I)$][a]	0.0710	0.0449	0.0537	0.0451	0.0575	0.0719
s[b]	1.011	0.987	1.009	0.991	0.981	1.075
Residual density [e Å^{-3}]	0.897/–0.517	0.238/–0.221	0.241/–0.255	0.219/–0.243	0.238/–0.271	0.558/–0.446

[a] Definition of the R indices: $R_1 = (\Sigma||F_o| - |F_c||)/\Sigma|F_o|$; $wR_2 = \{\Sigma[w(F_o^2 - F_c^2)^2]/\Sigma[w(F_o^2)^2]\}^{1/2}$ with $w^{-1} = \sigma^2(F_o^2) + (aP)^2 + bP$; $P = [2F_c^2 + \mathrm{Max}(F_o^2)]/3$. [b] $s = \{\Sigma[w(F_o^2 - F_c^2)^2]/(N_o - N_p)\}^{1/2}$.

Table 5. Crystal data and refinement details for the X-ray structure determinations of **7**–**10**.

Compound	**7**	**8**	**9**	**10**
Empirical formula	$C_{30}H_{56}N_6Na_2$	$C_{34}H_{64}K_2N_2O_8$	$C_{52}H_{62}N_3Na_3O_8{\cdot}C_4H_8O_2$	$C_{26}H_{40}N_2Na_2O_4{\cdot}2C_4H_8O$
Formula mass [g mol^{-1}]	546.79	707.07	1014.12	634.79
T [K]	–140(2)	–90(2)	–140(2)	–140(2)
Crystal system	triclinic	monoclinic	triclinic	monoclinic
Space group	$P\bar{1}$	$C2/c$	$P\bar{1}$	$P2_1/c$
a [Å]	9.4257(7)	18.8436(7)	11.0429(4)	10.4556(6)
b [Å]	9.4573(9)	13.9478(5)	13.0158(5)	16.3367(7)
c [Å]	10.7951(9)	16.3747(7)	19.3149(6)	10.7937(7)
α [°]	65.001(5)	90	83.064(2)	90
β [°]	72.783(5)	106.438(2)	79.563(2)	97.031(3)
γ [°]	77.745(6)	90	82.125(2)	90
V [Å^3]	828.83(12)	4127.8(3)	2691.35(16)	1829.81(18)
Z	1	4	2	2
ρ [g cm^{-3}]	1.095	1.138	1.251	1.152
μ [mm^{-1}]	0.88	2.74	1.05	0.98
Measured data	5611	14312	19652	12596
Data with $I > 2\sigma(I)$	2429	3224	6995	2070
Unique data (R_{int})	3681/0.0332	4718/0.0400	12232/0.0454	4173/0.1143
wR_2 (all data, on F^2)[a]	0.1859	0.1293	0.1349	0.2250
R_1 [$I > 2\sigma(I)$][a]	0.0609	0.0456	0.0563	0.0794
S[b]	1.052	1.033	1.008	1.021
Residual density [e Å^{-3}]	0.517/–0.273	0.378/–0.386	0.531/–0.598	0.811/–0.603

[a] Definition of the R indices: $R_1 = (\Sigma||F_o| - |F_c||)/\Sigma|F_o|$; $wR_2 = \{\Sigma[w(F_o^2 - F_c^2)^2]/\Sigma[w(F_o^2)^2]\}^{1/2}$ with $w^{-1} = \sigma^2(F_o^2) + (aP)^2 + \mathrm{bP}$; $P = [2F_c^2 + \mathrm{Max}(F_o^2)]/3$. [b] $s = \{\Sigma[w(F_o^2 - F_c^2)^2]/(N_o - N_p)\}^{1/2}$.

10), -840069 (for **11**), -840070 (for **13**), and -840071 (for **14**) contain the supplementary crystallographic data for this paper. These data can be obtained free of charge from The Cambridge Crystallographic Data Centre via www.ccdc.cam.ac.uk/data_request/cif.

Supporting Information (see footnote on the first page of this article): Representations of molecular structures and numbering schemes of those compounds not shown here.

Acknowledgments

We thank the German Research Foundation (Deutsche Forschungsgemeinschaft, DFG, Bonn/Germany) for generously funding this research initiative. We are also grateful to Alexander and Daniel Schmidt and Stephan Sinn for their support as part of an advanced laboratory course.

Table 6. Crystal data and refinement details for the X-ray structure determinations of **11**–**14**.

Compound	**11**	**12**	**13**	**14**
Empirical formula	C_7H_8KN	$C_{65}H_{100}K_5N_5O_5{\cdot}C_4H_8O$	$C_{22}H_{32}K_2N_2O$	$C_{20}H_{29}K_2N_2O$
Formula mass [g mol^{-1}]	145.24	1299.10	418.70	391.65
T [K]	–90(2)	–90(2)	–90(2)	–90(2)
Crystal system	rhombohedral	triclinic	triclinic	triclinic
Space group	$R\bar{3}$	$P\bar{1}$	$P\bar{1}$	$P\bar{1}$
a [Å]	19.8307(6)	15.4182(5)	9.4586(6)	9.4064(12)
b [Å]	19.8307(6)	15.5002(5)	11.3654(8)	10.3596(12)
c [Å]	34.2982(13)	18.0095(6)	12.0870(5)	12.0414(17)
α [°]	90.00	84.761(2)	69.923(4)	74.692(6)
β [°]	90.00	84.221(2)	74.765(4)	70.217(6)
γ [°]	120.00	80.1360(10)	89.180(3)	80.756(6)
V [Å^3]	11680.9(7)	4206.8(2)	1173.38(12)	1061.7(2)
Z	54	2	2	2
ρ [g cm^{-3}]	1.115	1.026	1.185	1.225
μ [mm^{-1}]	5.34	3.04	4.17	4.56
Measured data	15232	29987	8306	7451
Data with $I > 2\sigma(I)$	3745	10737	3050	2656
Unique data (R_{int})	5158/0.0400	19159/0.0349	5301/0.0388	4809/0.0445
wR_2 (all data, on F^2)[a]	0.2949	0.3419	0.1323	0.1185
R_1 [$I > 2\sigma(I)$][a]	0.0837	0.1023	0.0524	0.0531
S[b]	1.082	1.134	0.989	0.968
Residual density [e Å^{-3}]	0.953/–0.791	1.314/–0.694	0.484/–0.360	0.293/–0.288

[a] Definition of the R indices: $R_1 = (\Sigma||F_o| - |F_c||)/\Sigma|F_o|$; $wR_2 = \{\Sigma[w(F_o^2 - F_c^2)^2]/\Sigma[w(F_o^2)^2]\}^{1/2}$ with $w^{-1} = \sigma^2(F_o^2) + (aP)^2 + bP$; $P = [2F_c^2 + \mathrm{Max}(F_o^2)]/3$. [b] $s = \{\Sigma[w(F_o^2 - F_c^2)^2]/(N_o - N_p)\}^{1/2}$.

[1] a) M. F. Lappert, P. P. Power, A. R. Sanger, R. C. Srivastava, *Metal and Metalloid Amides*, Ellis Horwood, Chichester, **1980**, chapter 2, pp. 24–44; b) R. E. Mulvey, *Chem. Soc. Rev.* **1991**, *20*, 167–209; c) K. Gregory, P. v. R. Schleyer, R. Snaith, *Adv. Inorg. Chem.* **1991**, *37*, 47–142; d) D. B. Collum, *Acc. Chem. Res.* **1992**, *25*, 448–454; e) D. B. Collum, *Acc. Chem. Res.* **1993**, *26*, 227–234; f) F. Pauer, P. P. Power, *Lithium Chemistry: A Theoretical and Experimental Overview* (Eds.: A.-M. Sapse, P. v. R. Schleyer) Wiley, New York, **1995**, pp. 295–392.

[2] M. Lappert, A. Protchenko, P. P. Power, A. Seeber, *Metal Amide Chemistry*, Wiley, Chichester, **2009** and references cited therein.

[3] a) W. Vargas, U. Englich, K. Ruhlandt-Senge, *Inorg. Chem.* **2002**, *41*, 5602–5608; b) M. Gillett-Kunnath, W. Teng, W. Vargas, K. Ruhlandt-Senge, *Inorg. Chem.* **2005**, *44*, 4862–4870; c) M. Gärtner, R. Fischer, J. Langer, H. Görls, D. Walther, M. Westerhausen, *Inorg. Chem.* **2007**, *46*, 5118–5124; d) M. Gärtner, H. Görls, M. Westerhausen, *Inorg. Chem.* **2007**, *46*, 7678–7683; e) M. Gärtner, H. Görls, M. Westerhausen, *Dalton Trans.* **2008**, 1574–1582.

[4] C. Glock, H. Görls, M. Westerhausen, *Inorg. Chem.* **2009**, *48*, 394–399.

[5] C. Glock, H. Görls, M. Westerhausen, *Inorg. Chim. Acta* **2011**, *374*, 429–434.

[6] P. B. Hitchcock, Q.-G. Huang, M. F. Lappert, X.-H. Wei, *J. Mater. Chem.* **2004**, *14*, 3266–3273.

[7] G. R. Giesbrecht, G. E. Collis, J. C. Gordon, D. L. Clark, B. L. Scott, N. J. Hardman, *J. Organomet. Chem.* **2004**, *689*, 2177–2185.

[8] M. Gärtner, H. Görls, M. Westerhausen, *Organometallics* **2007**, *26*, 1077–1083.

[9] A. M. Johns, S. C. Chmely, T. P. Hanusa, *Inorg. Chem.* **2009**, *48*, 1380–1384.

[10] a) R. P. Davies, *Inorg. Chem. Commun.* **2000**, *3*, 13–15; b) A. R. Kennedy, R. E. Mulvey, R. B. Rowlings, *J. Organomet. Chem.* **2002**, *648*, 288–292; c) X. He, B. C. Noll, A. Beatty, R. E. Mulvey, K. W. Henderson, *J. Am. Chem. Soc.* **2004**, *126*, 7444–7445.

[11] C. Glock, H. Görls, M. Westerhausen, *Dalton Trans.* **2011**, *40*, 8108–8113.

[12] a) C. R. Hauser, H. G. Walker, *J. Am. Chem. Soc.* **1947**, *69*, 295–297; b) C. R. Hauser, F. C. Frostick, *J. Am. Chem. Soc.* **1949**, *71*, 1350–1352.

[13] An excellent review on alkali-metal-based deprotonation reagents is given in: R. E. Mulvey, *Acc. Chem. Res.* **2009**, *42*, 743–755.

[14] P. E. Eaton, C.-H. Lee, Y. Xiong, *J. Am. Chem. Soc.* **1989**, *111*, 8016–8018.

[15] L. Gupta, A. C. Hoepker, K. J. Singh, D. B. Collum, *J. Org. Chem.* **2009**, *74*, 2231–2233.

[16] a) P. García-Álvarez, D. V. Graham, E. Hevia, A. R. Kennedy, J. Klett, R. E. Mulvey, C. T. O'Hara, S. Weatherstone, *Angew. Chem.* **2008**, *120*, 8199–8201; *Angew. Chem. Int. Ed.* **2008**, *47*, 8079–8081; b) D. R. Armstrong, P. García-Álvarez, A. R. Kennedy, R. E. Mulvey, J. A. Parkinson, *Angew. Chem.* **2010**, *122*, 3253–3256; *Angew. Chem. Int. Ed.* **2010**, *49*, 3185–3188; c) M. Jaric, B. A. Haag, A. Unsinn, K. Karaghiosoff, P. Knochel, *Angew. Chem.* **2010**, *122*, 5582–5586; *Angew. Chem. Int. Ed.* **2010**, *49*, 5451–5455.

[17] a) R. E. Mulvey, *Chem. Commun.* **2001**, 1049–1056; b) M. Driess, R. E. Mulvey, M. Westerhausem, *Molecular Clusters of the Main Group Elements* (Eds. M. Driess, H. Nöth), Wiley-VCH, Weinheim, **2004**, pp. 391–424; c) R. E. Mulvey, *Organometallics* **2006**, *25*, 1060–1075; d) R. E. Mulvey, F. Mongin, M. Uchiyama, Y. Kondo, *Angew. Chem.* **2007**, *119*, 3876–3899; *Angew. Chem. Int. Ed.* **2007**, *46*, 3802–3824; e) C. J. Rohbogner, S. H. Wunderlich, G. C. Clososki, P. Knochel, *Eur. J. Org. Chem.* **2009**, 1781–1795.

[18] P. Hubberstey, *Coord. Chem. Rev.* **1988**, *85*, 1–85.

[19] M. Gärtner, H. Görls, M. Westerhausen, *Acta Crystallogr., Sect. E* **2007**, *63*, m2287.

[20] M. Gärtner, H. Görls, M. Westerhausen, *Acta Crystallogr., Sect. E* **2007**, *63*, m2289.

[21] A. R. Kennedy, J. Klett, C. T. O'Hara, R. E. Mulvey, G. M. Robertson, *Eur. J. Inorg. Chem.* **2009**, 5029–5035.

[22] P. B. Hitchcock, A. V. Khvostov, M. F. Lappert, A. V. Protchenko, *J. Organomet. Chem.* **2002**, *647*, 198–204.

[23] $[(L)_mAN(SiMe_3)_2]_n$: a) P. G. Williard, M. A. Nichols, *J. Am. Chem. Soc.* **1991**, *113*, 9671–9673, where A = K; L = 2thf and (thf)NaN(SiMe$_3$)$_2$; m = 1, n = 1 and A = Na, K; L = 2thf and (thf)LiN(SiMe$_3$)$_2$; m = 1, n = 1; b) F. T. Edelmann, F. Pauer,

M. Wedler, D. Stalke, *Inorg. Chem.* **1992**, *31*, 4143–4146, where A = Na; L = 1,4-diox; m = 1; $n = \infty$ and A = Rb, Cs; L = 1,4-diox; $m = 1.5$; $n = \infty$; c) M. Niemeyer, P. P. Power, *Organometallics* **1996**, *15*, 4107–4109, where A = Na; L = $AlMe_3$; $m = 2$; $n = 1$); d) J. Knizek, I. Krossing, H. Nöth, H. Schwenk, T. Seifert, *Chem. Ber./Recueil* **1997**, *130*, 1053–1062, where A = Na; no L; $n = -3$; e) M. Driess, H. Pritzkow, M. Skipinski, U. Winkler, *Organometallics* **1997**, *16*, 5108–5112, where A = Na; no L; $n = 3$; f) K. W. Henderson, A. E. Dorigo, Q.-L. Liu, P. G. Williard, *J. Am. Chem. Soc.* **1997**, *119*, 11855–11863, where A = Na; L = $(Me_2NCH_2)_2CH_2$; $m = 1$; $n = \infty$; g) M. Karl, G. Seybert, W. Massa, K. Harms, S. Agarwal, R. Maleika, W. Stelter, A. Greiner, W. Heitz, B. Neumüller, K. Dehnicke, *Z. Anorg. Allg. Chem.* **1999**, *625*, 1301–1309, where A = Na; L =thf; $m = 1$; $n = 2$; h) S. Neander, U. Behrens, *Z. Anorg. Allg. Chem.* **1999**, *625*, 1429–1434, where A = Cs; no L; $n = 2$; i) G. C. Forbes, A. R. Kennedy, R. E. Mulvey, P. J. A. Rodger, *Chem. Commun.* **2001**, 1400–1401, where A = Na; L = *O*-tmp; $m = 1$; $n = 2$; j) O. Schmitt, G. Wolmershäuser, H. Sitzmann, *Eur. J. Inorg. Chem.* **2003**, 3105–3109, where A = Na; L = $(C_5HiPr_4)_2LnCl$ with Ln = Pr, Nd; $m = 1$; $n = 2$; k) M. Westerhausen, S. Weinrich, B. Schmid, S. Schneiderbauer, M. Suter, H. Nöth, H. Piotrowski, *Z. Anorg. Allg. Chem.* **2003**, *629*, 625–633, where A = Cs; L = $[CsP(H)SitBu_3]_2$, $m = 1$, $n = 2$; l) C. Knapp, E. Lork, T. Borrmann, W.-D. Stohrer, R. Mews, *Z. Anorg. Allg. Chem.* **2005**, *631*, 1885–1892, where A = Na; L = *t*Bu-CN; $m = 1$; $n = 2$; m) A. G. Avent, F. Antolini, P. B. Hitchcock, A. V. Khvostov, M. F. Lappert, A. V. Protchenko, *Dalton Trans.* **2006**, 919–927, where A = Na; L = Ad-CN, *t*Bu-CN; $m = 1$; $n = 2$; n) Y. Sarazin, S. J. Coles, D. L. Hughes, M. B. Hursthouse, M. Bochmann, *Eur. J. Inorg. Chem.* **2006**, 3211–3220, where A = Na; L =thf; $m = 0.5$; $n = 2$; o) T. W. Hudnall, C. W. Bielawski, *J. Am. Chem. Soc.* **2009**, *131*, 16039–16041, where A = Na; L = ketone; $m = 1$; $n = 2$.

[24] J. D. Smith, *Adv. Organomet. Chem.* **1998**, *43*, 267–348.

[25] D. R. Armstrong, P. García-Álvarez, A. R. Kennedy, R. E. Mulvey, S. D. Robertson, *Chem. Eur. J.* **2011**, *17*, 6725–6730.

[26] D. Barr, W. Clegg, L. Cowton, L. Horsburgh, F. M. Mackenzie, R. E. Mulvey, *J. Chem. Soc., Chem. Commun.* **1995**, 891–892.

[27] a) D. Hoffmann, W. Bauer, F. Hampel, N. J. R. van Eikema Hommes, P. v. R. Schleyer, P. Otto, U. Pieper, D. Stalke, D. S. Wright, R. Snaith, *J. Am. Chem. Soc.* **1994**, *116*, 528–536; b) M. Westerhausen, W. Schwarz, *Z. Naturforsch. B* **1998**, *53*, 625–627; c) M. G. Davidson, D. Garcia-Vivo, A. R. Kennedy, R. E. Mulvey, S. R. Robertson, *Chem. Eur. J.* **2011**, *17*, 3364–3369.

[28] S. Harder, *Z. Anorg. Allg. Chem.* **2010**, *636*, 2205–2211.

[29] *COLLECT*, Data Collection Software, Nonius B. V., Netherlands, **1998**.

[30] Z. Otwinowski, W. Minor, *Methods in Enzymology*, vol. 276 ("Macromolecular Crystallography", Part A) (Eds.: C. W. Carter, R. M. Sweet), Academic Press, New York, **1997**, pp. 307–326.

[31] G. M. Sheldrick, *Acta Crystallogr., Sect. A* **2008**, *64*, 112–122.

Received: August 22, 2011
Published Online: October 31, 2011

